**Atmospheric
Chemistry
and Physics
Discussions**

ACPD

5, 4477–4505, 2005

**Refining temperature
in TOT/TOR analysis**

J. C. Chow et al.

Title Page

Abstract	Introduction
Conclusions	References
Tables	Figures

◄◄	►►
◄	►
Back	Close

Full Screen / Esc

Print Version

Interactive Discussion

EGU

Refining temperature measures in thermal/optical carbon analysis

J. C. Chow[1], **J. G. Watson**[1], **L.-W. A. Chen**[1], **G. Paredes-Miranda**[1],
M.-C. O. Chang[1], **D. Trimble**[1], **K. Fung**[2], **H. Zhang**[3], **and J. Z. Yu**[3]

[1]Division of Atmospheric Sciences, Desert Research Institute, 2215 Raggio Parkway, Reno,
NV 89512, USA
[2]Atmoslytic Inc., 24801 Alexandra Ct., Calabasas, CA 91302, USA
[3]Department of Chemistry, Hong Kong University of Science and Technology, Clear Water
Bay, Hong Kong, China

Correspondence to: J. C. Chow (judy.chow@dri.edu)

Title Page

Abstract | Introduction

Conclusions | References

Tables | Figures

|◀ | ▶|

◀ | ▶

Back | Close

Full Screen / Esc

Print Version

Interactive Discussion

EGU

Abstract

The thermal/optical method has been widely used for quantifying total carbon (TC), organic carbon (OC), and elemental carbon (EC) content in ambient and source particulate samples. Thermally defined carbon fractions have been used for source identification. Temperature precision in thermal carbon analysis is critical to the allocation of carbon fractions. The sample temperature is determined by a thermocouple, which is usually located in the oven near the sample punch, and which may be biased due to different thermal properties between the sample filter punch and the thermocouple, or the inhomogeneity in the heating zone. Quick-drying temperature-indicating liquids (Tempil Inc., South Plainfield, NJ) of different liquefying points are used as temperature calibration standards. These temperature indicators consist of chemicals that change their appearance at specific temperatures, and can be optically monitored to determine the sample temperature. Temperature measures were evaluated for three different models of carbon analyzers. The actual sample temperature was frequently underestimated by 10 to 50°C in all three analyzers. This experiment allowed calibration curves to be constructed that relate the sample temperature to the temperature measured by a thermocouple. Even though temperature variations of up to 50°C do not alter the OC and EC concentrations, a positive bias of 14 to 22°C during thermal analysis can significantly change carbon fraction measurements.

1. Introduction

Carbonaceous aerosol plays a major role in air pollution, visibility, health, and climate effects (e.g., Chow et al., 2005; Watson, 2002; Vedal, 1997; Jacobson 2001). Atmospheric carbon consists of: organic carbon (OC, including various organic compounds), elemental carbon (EC, or black carbon [BC]/soot, a non-volatile/light-absorbing carbon), and a small quantity of carbonate carbon (e.g., $CaCO_3$; Chow and Watson, 2002; Cao et al., 2004).

Heating of solid materials and detection of the evolved gases has been used since the time of Lavoisier (1789) to determine the composition of those materials. Differential and evolved gas analyses were staples of the analytical chemist (MacKenzie, 1970) until the latter part of the 20th century when other instrumentation became available.

5   Thermal evolution methods are still in widespread use today (Watson et al., 2005) to measure total carbon (TC=OC+EC) and fractions in suspended particles collected on filters that are classified as OC and EC. OC, EC, and other carbon fractions are defined by the temperatures at which they evolve, sometimes in conjunction with optical detection of BC. Precise measures of the sample temperature are difficult to obtain owing

10 to different locations and heating characteristics of the sample and the temperature sensor. This difference between sample and temperature sensors could be one of the causes of differences between OC and EC measurements by different laboratories applying similar thermal evolution methods (e.g., Currie et al., 2002; Schmid et al., 2001; Watson et al., 2005). These temperature differences may be especially important when

15 data are compared from different networks such as the non-urban Interagency Monitoring of Protected Visual Environments network (IMPROVE, Chow et al., 1993, 2001, 2004a) and urban Speciation Trends Network (STN, Peterson and Richards, 2002) in the United States. Hundreds of thousands of carbon measurements have been acquired in these networks that are used for air quality planning and research purposes.

20 Thermally-derived carbon fractions that are quite sensitive to the evolution temperature have recently been found useful for estimating the source contributions to suspended particulate matter (PM) (Chow et al., 2004b; Kim and Hopke, 2004a, b, c; Kim et al., 2004; Lee et al., 2003; Maykutt et al., 2003; Strezov et al., 2003; Zhao and Hopke et al., 2004).

25 This paper describes a method applicable to thermal analysis with optical detection that allows temperature sensors to be calibrated against actual sample temperatures. The method is applied to estimate deviation of "target" (i.e., protocol sample) from "measured" (i.e., thermocouple) temperatures for the Desert Research Institute/Oregon Graduate Center Carbon Analyzer (DRI/OGC, Desert Research Insti-

tute, Reno, NV); DRI Model 2001 thermal/optical carbon analyzer (Atmoslytic Inc., Calabasas, CA); and the Sunset Laboratory Carbon Aerosol Analysis Laboratory Instrument (Sunset Laboratory, Tigard, OR) to quantify the temperature biases in the current experimental configurations. The effects of these biases from target temperatures on
5 OC, EC, and thermally-derived carbon fractions are examined. An algorithm is developed using the calibrations to reconcile the target and measured temperatures. Use of this calibration method is expected to allow deviations between laboratories to be better understood, permit study of thermally-derived carbon fractions that might better represent source contributions, and obtain better precision on OC, EC, and carbon
10 fraction measurements.

2. Experimental apparatus and procedure

2.1. Thermal analysis methods

OC and EC are removed from sampling substrates (e.g., quartz-fiber filter) by volatilization, and/or combustion at selected temperatures, and by conversion of the released
15 gases to carbon dioxide (CO_2) or methane (CH_4), followed by infrared absorption (CO_2) or flame ionization (CH_4) detection (Novakov, 1982; Huntzicker et al., 1982; Chow et al., 1993; Turpin et al., 1994; Birch and Cary, 1996). EC is not volatile and is only released by oxidation, typically in an oxygen-containing atmosphere at a temperature above 340°C (Cachier et al., 1989). Most OC is expected to volatilize in an oxygen-
20 free environment below 550°C; therefore, it can be separated from EC. Heating in an inert atmosphere, however, causes certain OC compounds to pyrolyze or char, thereby inflating the atmospheric EC in the sample. In thermal/optical carbon analysis (e.g., Chow et al., 2001), a red light laser monitors the darkening of the particle deposit on the filter due to OC charring. When the reflected or transmitted light attains its origi-
25 nal intensity, the pyrolyzed OC (i.e., OP) is considered to have been removed and the remaining carbon is assumed to be the EC that was originally on the filter. Although

Refining temperature in TOT/TOR analysis

J. C. Chow et al.

the principles of thermal methods appear to be similar, they contain subtle variations with respect to: location of the temperature monitor (i.e., thermocouple) relative to the sample; analysis atmospheres; temperature ramping rates; temperature plateaus; residence time at each plateau; optical pyrolysis monitoring configuration; carrier gas flow
[5] through or across the sample; and oven flushing conditions. These differences are not always well characterized or reported with the analysis results.

The rate of OC volatilization or EC oxidation reaction kinetics can be described by the Arrhenius (1889) equation:

$$-\frac{1}{[C]} \sum_i \frac{d[C]}{dt}\bigg|_i = \sum_i k_i = \sum_i A_i \times \exp\left(\frac{-E_{a,i}}{RT}\right), \tag{1}$$

[10] where: $[C]$=total carbon compound concentration, i=reaction of mechanism dependent chemical species, k_i=rate constant for reaction i, A_i=dynamic constant for reaction i, $E_{a,i}$=activation energy for reaction i, R=universal gas constant (8.314×10^{-3} kJ mol^{-1}K^{-1}), and T=temperature (°K), where the reaction rate k_i (volatilization, pyrolysis, oxidation, etc.) decreases exponentially with the inverse of
[15] temperature. A significant change in reaction rate occurs as the temperature approaches that of the activation energy (i.e, $E_{a,i}/R$), which differs for different chemical compounds. The temperature program influences the evolution of OC and EC, and possibly the OC/EC split (Chow et al., 2001, 2004a). The rates and quantities of carbon leaving the sample at different temperatures reflect the composition of car-
[20] bonaceous material in the sample (Chow et al., 2005; Currie et al., 2002). In addition to OC and EC, temperature-resolved carbon fractions have been reported from major ambient networks. For example, the IMPROVE network for the United States National Parks and Wildlife Reserves reports eight carbon fractions between 120°C and 800°C (Table 1) since the commencement of the project in 1988. More recently, the STN ap-
[25] plied in urban areas in the United States also reports four sub-fractions of OC resolved by the analysis temperature program (Table 1).

Refining temperature in TOT/TOR analysis

J. C. Chow et al.

Title Page

Abstract	Introduction
Conclusions	References
Tables	Figures

⏮ | ⏭

◀ | ▶

Back | Close

Full Screen / Esc

Print Version

Interactive Discussion

EGU

2.2. Carbon analyzers

The DRI/OGC analyzers have been used for thermal/optical reflectance (TOR) analysis of quartz-fiber filter samples acquired from the IMPROVE network and other ambient and source characterization studies since 1986 following the IMPROVE TOR char-

5 ring correction protocol (Chow et al., 1993). The Sunset analyzer implements thermal/optical transmission (TOT) charring correction for the NIOSH (1999), STN (Peterson and Richards, 2002), and the Hong Kong University of Science and Technology (HKUST-3) (Yang and Yu, 2002) thermal protocols. The Model 2001 analyzer implements both the TOR and TOT charring correction for all temperature protocols. The IM-

10 PROVE, STN, and HKUST-3 temperature protocols are documented in Table 1. Three configurations of instruments are compared in Table 2. Figure 1 illustrates the location of the temperature sensors relative to the sample. Thermocouples do not contact the sample punch in any of the instruments. Sample temperatures may differ from the thermocouple temperature due to: 1) different thermal properties of the sample and

15 thermocouple; 2) temperature gradients in the sample oven; and/or 3) temperature gradients between the sample oven and the oxidation oven.

The DRI/OGC analyzer uses a Nichrome heating coil (Marchi Associates, SDH 175, Redwood City, CA) that is partially exposed to the ambient air without insulation. The temperature gradient in the sample heating zone varies from ~20°C/cm at 1% power

20 output to ~50°C/cm at 75% power output (>600°C). A shielded Omega type- K thermocouple (Stamford, CT) serves as both a temperature sensor and a pushrod, to which the sample holder is attached. Sample punches are loaded and manually inserted into the heating zone. The thermocouple tip is loosely separated from the sample punch by 2 to 4 mm (Fig. 1a). The ungrounded type-K thermocouple requires approximately

25 18 s to equilibrate its response to a given temperature plateau.

In the Model 2001 analyzer, the sample punch is placed in a quartz holder oriented parallel to the direction of the carrier gas flow. Sample insertion is controlled by an electric stepper motor that ensures a repeatable sample position in the oven by a pushrod

Title Page

Abstract	Introduction
Conclusions	References
Tables	Figures

◄◄	►►
◄	►
Back	Close

Full Screen / Esc

Print Version

Interactive Discussion

EGU

containing the thermocouple. The external shield for this grounded type-K thermocouple is removed to reduce the response time to less than one second, and the sensor tip is located <2 mm under the edge of the filter punch to minimize interference with the reflectance and transmittance measurements (Fig. 1b). Two iron-chromium-aluminum

5 (ICA) heaters are insulated by firebrick blocks to avoid heat dissipation. The temperature sensor is always in the same position relative to the sample, and the sample is in the same part of the oven, until the thermocouple is replaced.

The Sunset analyzer locates the sample punch on a transparent quartz spatula that is placed at the same location in the oven. The sample holder has a flat (2 cm^2) surface

10 at one end to hold a filter sample and a long stem to facilitate the manual loading of the filter sample into the oven. The quartz oven, which is enclosed in a case insulated with quartz wool and pads, is wrapped by a Nichrome heating coil (Sciare et al., 2003). As shown in Fig. 1c, the thermocouple is in a fixed location ~20 mm downstream of the filter punch center. The sample is placed between two stops on the flat end of the

15 sample holder to ensure its precise position.

In each instrument, the evolved carbon is first converted to CO_2 through an oxidizer (manganese dioxide [MnO_2] at ~900°C). The CO_2 is then reduced to CH_4 as the carrier gas passes through a granulated firebrick impregnated with nickel catalyst at ~400°C. The CH_4 is then quantified by a flame ionization detector (FID). The FID is operated

20 at a time resolution of one second. The same type of red light (632.8 nm) helium-neon laser is used for charring correction among the three different models of carbon analyzers.

2.3. Temperature indicators

Since it is not possible to sense the temperature of the sample directly, materials were

25 sought that: 1) could be placed where the sample would normally be located and 2) would cause sharp reactions when known temperatures were achieved. Metallic melting point standards (e.g., tin at 232°C and zinc at 420°C) exhibit sharp changes in heat capacity, conductivity, and/or viscosity at their phase transition points; however, these

Refining temperature in TOT/TOR analysis

J. C. Chow et al.

EGU

properties cannot be detected by the FID or optics. Organic melting point standards rely on the change in vapor pressure at the phase transition point, and this change can be detected by the FID; however, these compounds often evaporate or sublimate prior to boiling, thereby smearing the FID response. The FID response is further diffused as
5 it passes through the oxidation and reduction ovens.

Quick-drying temperature-indicating liquids of different melting points, Tempilaq° G (Tempil Inc., South Plainfield, NJ, USA), are used as temperature indicators in muffle furnaces. A Tempilaq° G set contains long-chain hydrocarbons, suspended in an organic solvent, which change their appearance at 44 specific temperatures spanning
10 80 to 1100°C. The accuracy of Tempilaq° G is certified within ±1% of its designated temperature and is traceable to the National Institute of Standards and Technology (NIST). Tempilaq° G is bottled in liquid form and dries quickly to a dull, opaque film when applied to a surface. As the surface is heated to the designated temperature, the film liquefies and is accompanied by a change of appearance that can be optically
15 monitored to determine sample temperature.

2.4. Standard preparation

Temperature calibration requires a pre-fired quartz-fiber filter (#2500 QAT-UP, Pall Life Sciences, Ann Arbor, MI) punch ($0.5\,cm^2$ for DRI analyzers and $1.0\,cm^2$ for the Sunset analyzer) and a clean matching-sized quartz disk (Continental Glass Engineering, Bur-
20 bank, CA). Quartz-fiber filter punches are sliced in half with a filter-sectioning device (Fung et al., 2004). A thin layer of Tempilaq° G ($25\,\mu L$) is uniformly applied to the quartz disk surface with a 0.1 ml Eppendorf graduated Combitip (Brinkman Instruments Inc., Westbury, NY), and it is immediately (before drying) covered with a sliced filter punch. For cost savings, a glass – instead of quartz – disk can be used for Temiplaq° G at
25 temperatures less than 520°C. The disk sandwich (i.e., temperature standard) is then loaded into the sample holder for analysis. The mass of applied Tempilaq° G can be determined gravimetrically, and it varies from 8 to 31 mg for different temperature indicators due to varying liquid densities. For a given temperature level of Tempilaq° G, the

precision of its mass was ∼10% in these experiments.

2.5. Temperature Program

After insertion of the temperature standard into the analyzer, the temperature is slowly (2°C/min) ramped across a 50°C range containing the specified Tempilaq˚ G melt-
5 ing point. This slow ramping creates a quasi-equilibrium condition that allows the phase transition point to be resolved. When the specified temperature is reached, the Tempilaq˚ G liquefies, causing a sharp change in reflectance and transmittance.

Figure 2 demonstrates the thermocouple temperature, reflectance, and transmittance as a function of thermal analysis time. The reflectance and transmittance remain
10 relatively flat until the temperature approaches its specified value of 184°C. Figure 3 compares the time series of reflectance, transmittance, and their respective first- and second- order derivatives. The second-order derivative (change in the slope) records the inflection point of reflectance or transmittance that provides the best indication of the attainment of the designated temperature. Thermocouple temperature at this crit-
15 ical point is recorded as "measured" temperature. The temperature deviation (ΔT) between the sample and the thermocouple temperatures is determined by comparing the rated Tempilaq˚ G temperature with this measured value.

In the Model 2001, the reflectance-based method generally gives a lower liquefying temperature than the transmittance-based method, within ±2°C. Given the uncertainty
20 in the Tempilaq˚ G temperature rating of ±1%, calibrations based on the two optical methods are considered to be equivalent; therefore, their means are used. Among temperature indicators that achieve an adequate signal/noise ratio, the 121, 184, 253, 510, 649, 704, and 816°C mixtures were chosen for IMPROVE protocol temperature calibration, whereas 121, 184, 253, 510, 649, and 927°C mixtures were used for the
25 HKUST-3 protocol. Replicate analyses were performed to evaluate the precision of temperature deviations. Temperature deviations for all the instruments rarely exceeded 50°C across the tested temperature ranges, but they did vary appreciably among the

different instrument designs.

3. Analysis results and instrument variations

Five DRI/OGC (CA #1–#5), five DRI Model 2001 (CA #6–#11), and one Sunset analyzers were tested. Tables 3 to 5 summarize the average temperature deviations at each test temperature for the 11 analyzers. A positive temperature deviation indicates that the thermocouple sensor underestimates the sample temperature and vice-versa.

For the Model 2001 analyzers, the sample temperature was <10°C hotter than the sensor reading at the lowest two temperatures (<200°C), and increased to 20 to 30°C hotter at the higher temperatures. The precision of temperature deviations (i.e., $\sigma_{\Delta T}$), determined from the standard deviation of multiple replicate analyses, were generally within ±4°C. This reflects the consistency of analytical conditions among the five analyzers. Table 3 shows nearly linear relationships between the target and measured temperatures with high correlations. Thus, a constant temperature offset of 3 to 12°C can be applied in the carbon analyzer software to reflect target sample temperatures.

Temperature tests for DRI/OGC analyzers contain two analyses in which ΔT for both the maximum and minimum sample-to-thermocouple distances were determined. Table 4 shows that the sample temperature was 10 to 50°C hotter than the sensor readings at all temperature ranges, except for carbon analyzer (CA) #1, where a ΔT of 57–77°C was found for the highest temperature (704°C). Besides inter-analyzer differences, temperatures varied by more than 20°C in replicate tests for a given analyzer. This variability exceeds the uncertainty of Tempilaq˚G (±1%). The linear regression of rated Tempilaq˚G (target) temperature against thermocouple (measured) temperature yields slopes and intercepts that are associated with larger standard deviations (Table 4). According to Eq. (1), the effect of this temperature bias may be more pronounced at lower temperatures.

For the Sunset analyzer, the sample temperature was 12 to 33°C hotter than the sensor reading for the two lowest and highest temperatures, and 2 to 11°C cooler for

Refining temperature in TOT/TOR analysis

J. C. Chow et al.

the two middle temperatures. The good reproducibility (∼±3°C) for the Sunset and Model 2001 analyzers is sufficient to reveal differences between the target and measured temperatures.

4. Temperature calibration

5   Temperature bias during thermal carbon analysis can vary between different designs of instruments, within the same model of analyzer, and among replicate analyses. Periodic temperature calibration and performance testing is needed to achieve good reproducibility of carbon fraction measurements. Linear calibration curves can be generated, as illustrated in Fig. 4.

10   $$T_{sample(target)} = b \times T_{thermocouple(measured)} + a \,, \tag{2}$$

where $T_{sample(target)}$ is the set point temperature specified by the analytical protocols and $T_{thermocouple(measured)}$ is the sensor reading of a thermocouple. Variables a and b are the intercept and slope, respectively, and are determined from the least-square linear regression between the target and measured temperatures from the tests. Set-
15   point temperatures can be adjusted so that $T_{sample}=T_{thermocouple}$, or the software can be modified to accommodate the calibration. In either case, the temperature reported should reflect the sample temperature, not the thermocouple temperature.

Five ambient samples acquired from the Fresno Supersite (Watson et al., 2000; Chow et al., 2004) were analyzed by a Model 2001 analyzer with and without the
20   adjustment after the temperature calibration. These samples represent an urban environment where contributions from vegetative burning, cooking, gasoline and diesel vehicle exhaust, and secondary organic aerosol vary throughout the year (Poore, 2002; Schauer and Cass, 2000; Watson and Chow, 2002a, b; Watson and Chow, 2002; Watson et al., 2002a, b). TC concentrations of the five samples ranged from 3.5 to
25   15 μg m^{-3}. Figure 4 shows that $T_{thermocouple}$ underestimates T_{sample}; deviations from

Refining temperature in TOT/TOR analysis

J. C. Chow et al.

linearity suggest temperature inhomogeneity in the heating zone. Based on the temperature calibration results, the samples were re-analyzed using a modified IMPROVE protocol in which the temperature was lowered by 14 to 22°C. Figure 5 shows that while these temperature deviations did not change the OC/EC split for TOR or TOT, cooler
5 temperatures reduced the low temperature OC fractions (OC1–OC3) and increased the high temperature OC4 and EC fractions. After the adjustment based on temperature calibration, the average changes in OC1 (120°C) and EC2 (700°C) exceeded 30%, partially due to low carbon concentrations in these carbon fractions. OC1 represents semi-volatile organics, which are most likely sampling artifacts that result in substantial
10 variability. Charred OC (by reflectance or transmittance) increased by ~20% when the sample temperature was lowered by 14 to 22°C.

   Lower analysis temperatures (after calibration) did not change the OC/EC split, and the reduced OC1 and OC3 fractions were compensated by the inflated pyrolysis fraction. While carbon fraction measurements may vary between different analyzers due
15 to uncertain analysis temperatures, this study suggests that the OC/EC split through optical charring correction is less perturbed, at least for the IMPROVE TOR protocol. Transmittance-based charring correction may be more dependent on analysis temperatures owing to charring of adsorbed organic vapors within the filter that affect transmittance more than reflectance from the surface deposit (Chow et al., 2004a; Chen et
20 al., 2004).

5. Summary and conclusions

A method has been presented that can relate the sample temperature to the sensor temperature in thermal/optical carbon analyzers. It uses temperature-sensitive compounds that change their appearance when they reach a target temperature.
25 Five to six temperature indicators, covering a range of 120 to 930°C, were used to evaluate the temperature measures in three different carbon analyzer models: the DRI/OGC, DRI Model 2001, and Sunset analyzers. Thermocouple sensors in all of the

Refining temperature in TOT/TOR analysis

J. C. Chow et al.

EGU

models underestimated the sample temperature; however, the bias in the DRI Model 2001 tended to be smaller and more consistent (<10°C for temperatures <200°C and <20 to 30°C for higher temperatures). There was a linear relationship between target and measured temperatures, with high correlation. The DRI/OGC analyzer reported temperatures that were 10 to 50°C lower than the target sample temperatures and that varied by as much as 20°C for replicate analysis. The temperature bias in the Sunset analyzer was less than 30°C, but it did not appear to be linearly related to the target temperatures.

Even though temperature variations of up to 50°C do not appear to alter the OC and EC concentrations with the IMPROVE thermal protocol, they do change the abundances of different carbon fractions from thermal/optical analysis. When applied to ambient samples from the urban Fresno Supersite, a calibration that corrected for a 14 to 22°C positive bias resulted in changes greater than 30% in the IMPROVE protocol for low temperature OC (OC1 at 120°C) and high temperature EC (EC2 at 700°C) fractions. Refining temperature measures in thermal/optical analysis for trends networks is necessary to ensure the consistency of carbon fraction measurements. This will avoid misinterpretation of the data in the future. The techniques developed in this study can reduce variability in thermal/optical analysis and be systematized into procedures that are applicable to a wide variety of instruments.

EGU

References

Arrhenius, S.: Über die Reaktionsgeschwindigkeit bei der Inversion von Rohzucker durch Säuren, Z. Phys. Chem., 4(26), 226–248, 1889.

Birch, M. E. and Cary, R. A.: Elemental carbon-based method for monitoring occupational exposures to particulate diesel exhaust; Aerosol Sci. Technol. 25(3), 221–241, 1996.

Cachier, H., Bremond, M. P., and Buat-Ménard, P.: Thermal separation of soot carbon, Aerosol Sci. Technol., 10(2), 358–364, 1989.

Cao, J. J., Lee, S. C., Zhang, X. Y., Chow, J. C., An, Z. S., Ho, K. F., Watson, J. G., Fung, K. K., Wang, Y. Q., and Shen, Z. X.: Characterization of airborne carbonate over a site near Asian dust source regions during spring 2002 and its climatic and environmental significance, J. Geophys. Res., 110(D03203), 1–8, 2005.

Chen, L.-W. A., Chow, J. C., Watson, J. G., Moosmüller, H., and Arnott, W. P.: Modeling reflectance and transmittance of quartz-fiber filter samples containing elemental carbon particles: Implications for thermal/optical analysis, J. Aerosol Sci., 35(6), 765–780, 2004.

Chow, J. C. and Watson, J. G.: $PM_{2.5}$ carbonate concentrations at regionally representative Interagency Monitoring of Protected Visual Environment sites, J. Geophys. Res., 107(D21), ICC 6-1-ICC 6-9, 2002.

Chow, J. C., Watson, J. G., Lowenthal, D. H., Solomon, P. A., Magliano, K. L., Ziman, S. D., and Richards, L. W.: PM_{10} and $PM_{2.5}$ compositions in California's San Joaquin Valley, Aerosol Sci. Technol., 18, 105–128, 1993.

Chow, J. C., Watson, J. G., Crow, D., Lowenthal, D. H., and Merrifield, T.: Comparison of IMPROVE and NIOSH carbon measurements, Aerosol Sci. Technol., 34(1), 23–34, 2001.

Chow, J. C., Watson, J. G., Chen, L.-W. A., Arnott, W. P., Moosmüller, H., and Fung, K. K.: Equivalence of elemental carbon by Thermal/Optical Reflectance and Transmittance with different temperature protocols, Environ. Sci. Technol., 38(16), 4414–4422, 2004a.

Chow, J. C., Watson, J. G., Kuhns, H. D., Etyemezian, V., Lowenthal, D. H., Crow, D. J., Kohl, S. D., Engelbrecht, J. P., and Green, M. C.: Source profiles for industrial, mobile, and area sources in the Big Bend Regional Aerosol Visibility and Observational (BRAVO) Study, Chemosphere, 54(2), 185–208, 2004b.

Chow, J. C., Watson, J. G., Louie, P. K. K., Chen, L.-W. A., and Sin, D.: Comparison of $PM_{2.5}$ carbon measurement methods in Hong Kong, China, Environ. Poll., 137, 334–344, 2005.

Currie, L. A., Benner Jr., B. A., Cachier, H., Cary, R., Chow, J. C., Druffel, E. R. M., Eglinton, T.

Title Page

Abstract | Introduction

Conclusions | References

Tables | Figures

|◄ | ►|

◄ | ►

Back | Close

Full Screen / Esc

Print Version

Interactive Discussion

EGU

I., Gustafsson, Ö., Hartmann, P. C., Hedges, J. I., Kessler, J. D., Kirchstetter, T. W., Klinedinst, D. B., Klouda, G. A., Marolf, J. V., Masiello, C. A., Novakov, T., Pearson, A., Prentice, K. M., Puxbaum, H., Quinn, J. G., Reddy, C. M., Schmid, H., Slater, J. F., Watson, J. G., and Wise, S. A.: A critical evaluation of interlaboratory data on total, elemental, and isotopic carbon in the carbonaceous particle reference material, NIST SRM 1649a, J. Res. National Bureau Standards, 107(3), 279–298, 2002.

Fung, K., Chow, J. C., Watson, J. G., and Chen, L. Y. .: Determining Organic Carbon Adsorption on Quartz Fiber Filters by Sample Splitting and Thermal/Optical Analysis, Proceedings 13th World Clean Air and Environmental Protection Congress and Exhibition, London, UK, 26 August 2004, 2004.

Huntzicker, J. J., Johnson, R. L., Shah, J. J., and Cary, R. A.: Analysis of organic and elemental carbon in ambient aerosols by a thermal-optical method, in: Particulate Carbon: Atmospheric Life Cycle, edited by: Wolff, G. T. and Klimisch, R. L., Plenum Press, New York, NY, 79–88, 1982.

Jacobson, M. Z.: Strong radiative heating due to the mixing state of black carbon in atmospheric aerosols, Nature, 409, 695–697, 2001.

Kim, E. and Hopke, P. K.: Comparison between conditional probability function and nonparametric regression for fine particle source directions, Atmos. Environ., 38(28), 4667–4673, 2004a.

Kim, E. and Hopke, P. K.: Source apportionment of fine particles at Washington, DC, utilizing temperature-resolved carbon fractions, JAWMA, 54(7), 773–785, 2004b.

Kim, E. and Hopke, P. K.: Improving source identification of fine particles in a rural northeastern US area utilizing temperature-resolved carbon fractions, J. Geophys. Res., 109(D9), D09204, 2004c.

Kim, E., Hopke, P. K., and Edgerton, E. S.: Improving source identification of Atlanta aerosol using temperature resolved carbon fractions in positive matrix factorization, Atmos. Environ., 38(20), 3349–3362, 2004.

Lavoisier, A.: Chapter 7, in: Traite Elementaire de Chimie, Volume 2, Paris, France, 493–501, 1789.

Lee, P. K. H., Brook, J. R., Dabek-Zlotorzynska, E., and Mabury, S. A.: Identification of the major sources contributing to $PM_{2.5}$ observed in Toronto, Environ. Sci. Technol., 37 (21), 4831–4840, 2003.

MacKenzie, R. C.: Differential Thermal Analysis Vol. 1: Fundamental Aspects, Academic Press,

EGU

New York, NY, 1970.

Maykut, N. N., Lewtas, J., Kim, E., and Larson, T. V.: Source apportionment of $PM_{2.5}$ at an urban IMPROVE site in Seattle, Washington, Environ. Sci. Technol., 37(22), 5135–5142, 2003.

NIOSH: Method 5040 Issue 3 (Interim): Elemental carbon (diesel exhaust), in: NIOSH Manual of Analytical Methods, National Institute of Occupational Safety and Health, Cincinnati, OH, 1999.

Novakov, T.: Soot in the atmosphere, in: Particulate Carbon: Atmospheric Life Cycle, edited by: Wolff, G. T. and Klimisch, R. L., Plenum Press: New York, NY, 19–41, 1982.

Peterson, M. R. and Richards, M. H.: Thermal-optical-transmittance analysis for organic, elemental, carbonate, total carbon, and OCX2 in $PM_{2.5}$ by the EPA/NIOSH method, in: Proceedings, Symposium on Air Quality Measurement Methods and Technology-2002, edited by: Winegar, E. D. and Tropp, R. J., Air & Waste Management Association, Pittsburgh, PA, 83-1-83-19, 2002.

Poore, M. W.: Levoglucosan in $PM_{2.5}$ at the Fresno supersite, JAWMA, 52(1), 3–4, 2002.

Schauer, J. J. and Cass, G. R.: Source apportionment of wintertime gas-phase and particle-phase air pollutants using organic compounds as tracers, Environ. Sci. Technol., 34(9), 1821–1832, 2000.

Schmid, H. P., Laskus, L., Abraham, H. J., Baltensperger, U., Lavanchy, V. M. H., Bizjak, M., Burba, P., Cachier, H., Crow, D., Chow, J. C., Gnauk, T., Even, A., ten Brink, H. M., Giesen, K. P., Hitzenberger, R., Hueglin, C., Maenhaut, W., Pio, C. A., Puttock, J., Putaud, J. P., Toom-Sauntry, D., and Puxbaum, H.: Results of the "Carbon Conference" international aerosol carbon round robin test: Stage 1, Atmos. Environ., 35(12), 2111–2121, 2001.

Sciare, J., Cachier, H., Oikonomou, K., Ausset, P., Sarda-Esteve, R., and Mihalopoulos, N.: Characterization of carbonaceous aerosols during the MINOS campaign in Crete, July–August 2001: A multi-analytical approach, Atmos. Chem. Phys., 3, 1743–1757, 2003, SRef-ID: 1680-7324/acp/2003-3-1743.

Strezov, V., Moghtaderi, B., and Lucas, J. A.: Thermal study of decomposition of selected biomass samples, J. Thermal Anal. & Calorimetry, 72(3), 1041–1048, 2003.

Turpin, B. J., Huntzicker, J. J., and Hering, S. V.: Investigation of organic aerosol sampling artifacts in the Los Angeles Basin, Atmos. Environ., 28(19), Research & Development, 3061–3071, 1994

Vedal, S.: Critical review – Ambient particles and health: Lines that divide, JAWMA, 47(5),

Refining temperature in TOT/TOR analysis

J. C. Chow et al.

Title Page

Abstract	Introduction
Conclusions	References
Tables	Figures

⏮   ⏭

◀   ▶

Back   Close

Full Screen / Esc

Print Version

Interactive Discussion

EGU

551–581, 1997.

Watson, J. G.: Visibility: Science and regulation, JAWMA, 52(6), 628–713, 2002.

Watson, J. G. and Chow, J. C.: A wintertime $PM_{2.5}$ episode at the Fresno, CA, supersite, Atmos. Environ. 36(3), 465–475, 2002a.

5   Watson, J. G. and Chow, J. C.: Comparison and evaluation of in-situ and filter carbon measurements at the Fresno Supersite, J. Geophys. Res., 107(D21), ICC 3-1-ICC 3-15, 2002b.

Watson, J. G., Chow, J. C., Bowen, J. L., Lowenthal, D. H., Hering, S., Ouchida, P., and Oslund, W.: Air quality measurements from the Fresno Supersite, JAWMA 50(8), 1321–1334, 2000.

Watson, J. G., Chow, J. C., Lowenthal, D. H., Stolzenburg, M. R., Kreisberg, N. M., and Hering,
10   S. V.: Particle size relationships at the Fresno supersite, JAWMA, 52(7), 822–827, 2002.

Watson, J. G., Chow, J. C., and Chen, L.-W. A.: Summary of organic and elemental/black carbon analysis methods and intercomparisons, Aerosol and Air Quality Research , 5(1), 69–109, 2005.

Yang, H. and Yu, J. Z.: Uncertainties in charring correction in the analysis of elemental and
15   organic carbon in atmospheric particles by thermal/optical methods, Environ. Sci. Technol., 36(23), 5199–5204, 2002.

Zhao, W. X. and Hopke, P. K.: Source apportionment for ambient particles in the San Gorgonio wilderness, Atmos. Environ. 38(35), 5901–5910, 2004.

EGU

Table 1. Comparison of the IMPROVE, STN, and HKUST-3 thermal/optical analysis protocols.

Methods' Carrier Gas	Carbon Fraction	IMP_TOR/TOT[a] Temperature, Time	STN_TOT/TOR[a] Temperature, Time	HKUST-3_TOT[a] Temperature, Time
He-Purge		30°C, 90 s	30°C, 90 s	30°C, 90 s
He-1	OC1	120°C, 150–580 s[c]	310°C, 60 s	250°C, 150 s
He-2	OC2	250°C, 150–580 s	480°C, 60 s	550°C, 150 s
He-3	OC3	450°C, 150–580 s	615°C, 60 s	650°C, 150 s
He-4	OC4	550°C, 150–580 s	900°C, 90 s	850°C, 150 s
He-5		–	Cool Oven	Cool Oven
O_2/He-1[b]	EC1	550°C, 150–580 s	600°C, 45 s	650°C, 150 s
O_2/He-2	EC2	700°C, 150–580 s	675°C, 45 s	750°C, 150 s
O_2/He-3	EC3	800°C, 150–580 s	750°C, 45 s	850°C, 150 s
O_2/He-4		–	825°C, 45 s	890°C, 150 s
O_2/He-5		–	920°C, 45 s	–

EGU

Table 1. Continued.

[a]IMPROVE_TOR:
Thermal/optical reflectance analysis following the IMPROVE (Interagency Monitoring of Protected Visual Environments) protocol using DRI/OGC analyzers (Desert Research Institute, Reno, NV). IMPROVE_TOR does not advance from one temperature to the next until a well-defined carbon peak has evolved (Chow et al., 1993, 2001, 2004a). Filter reflectance is monitored throughout the analysis, pyrolyzed OC (OP) is defined as the carbon evolving between the introduction of oxygen (O_2) in the helium (He) atmosphere and the return of reflectance to its initial value (the OC/EC split). OP is reported as a positive value if the OC/EC split occurs after the introduction of O_2, and as a negative value if the OC/EC split occurs before O_2 is introduced. In either case, OC equals OC1+OC2+OC3+OC4+OP and EC equals EC1+EC2+EC3-OP. Eight well-defined fractions of carbon, including four OC fractions (OC1, OC2, OC3, and OC4), three EC fractions (EC1, EC2, and EC3), and OP are reported as part of the IMPROVE_TOR protocol.

IMPROVE_TOR/TOT Same as the IMPROVE_TOR protocol but using a DRI Model 2001 thermal/optical carbon analyzer (Atmoslytic, Calabasas, CA). The DRI Model 2001 performs charring corrections through both reflectance and transmittance and reports as OPR and OPT, respectively. Subsequently, OC and EC calculated from OPR (OPT) are referred to as OCR and ECR (OCT and ECT), respectively.

STN_TOR/TOT Thermal/optical transmission/reflectance analysis following the Speciation Trends Network (STN) protocol. Filter transmittance is monitored to split OC and EC (STN_TOT). With the DRI Model 2001 thermal/optical carbon analyzer (Atmoslytic, Calabasas, CA), reflectance can also be recorded during the STN analyses. The protocol that uses STN temperature plateaus but a reflectance split is referred to as STN_TOR. The STN protocol has a short and fixed residence times per temperature plateau and does not report distinguishable carbon fractions. The STN protocol is currently applied to the U.S. $PM_{2.5}$ Speciation Monitoring Network.

EGU

Table 1. Continued.

HKUST-3_TOT Thermal/optical transmission analysis following the HKUST-3 (Hong Kong University of Science and Technology, Clear Water Bay, Hong Kong, China) protocol using a Sunset Laboratory Carbon Aerosol Analysis Laboratory Instrument (Sunset Laboratory, Tigard, OR). The HKUST-3 transmittance protocol has short and fixed residence times per temperature plateau and does not usually report distinguishable carbon fractions.

[b]2% O_2 in He for IMPROVE and STN protocols, and 1% O_2 in He for HKUST-3 protocol.

[c]The residence time at each temperature in the IMPROVE protocol depends on when the flame ionization detector (FID) signal returns to the baseline to achieve well-defined carbon fractions.

Table 2. Intercomparisons between DRI/OGC, DRI Model 2001, and Sunset Laboratory thermal/optical carbon analyzers.

Parameters	DRI/OGC	DRI Model 2001	Sunset Laboratory
Orientation of sample filter	Vertical. Carrier gas flows against the filter.	Horizontal. Carrier gas flows parallel to the filter.	Horizontal. Carrier gas flows parallel to the filter.
Sample size	$0.5\ cm^2$ circular punch	$0.5\ cm^2$ circular punch	$1\ cm^2$ rectangular punch
Thermocouple	Shielded Omega Type K thermocouple. Sheath diameter 0.32 cm Response time constant is ~ 18 seconds.	Unshielded (exposed) Omega Type K thermocouple. Sheath diameter 0.32 cm. Response time constant is <1 second.	Shielded Omega Type K thermocouple. Sheath diameter 0.16 cm. Response time constant is ~ 4 seconds.
Position of the thermocouple	Thermocouple is located 2 – 4 mm behind the center of sample punch and moves with the sample.	Thermocouple is located <2 mm underneath the filter punch and within 1 mm of the center of the punch. Thermocouple moves with the sample.	Thermocouple is located ~ 20 mm in front of the sample punch and fixed in the oven.
Oven design	Quartz oven. Perpendicular connection between the sample and the oxidation oven. The oven pressure is ~ 1 PSI.	Quartz oven. Straight connection between the sample and oxidation oven. A flow-limiting orifice installed between the sample and oxidation oven minimizes backflow from the catalyst. The oven pressure is ~ 3 PSI.	Quartz oven. Straight connection between the sample and the oxidation oven. A flow-limiting orifice installed between the sample and oxidation oven. Oven pressure is ~ 3 PSI.
Heater design	Quartz oven wrapped with custom-made 650 W Nichrome coiled heater (75 mm length x 18 cm outside diameter), with a large (300 mm length x 190 mm width x 190 mm depth) firebrick block as insulator. Coil is partially exposed to the air. Maximum ramping rate is ~ 5°C/min.	Two iron-chromium-aluminum (ICA) heaters imbedded in firebrick blocks (63 cm length x 25 cm width x 7.27 mm depth) shield both sides of the oven. A cooling fan is installed under the oven. Maximum ramping rate is ~ 7°C/min.	Quartz oven wrapped with heating coils and enclosed in a case with insulating quartz wool and pads. Maximum ramping rate is ~ 5°C/min.
Optical monitoring	Monitoring reflectance of sample relative to the initial (blank) value.	Monitoring both reflectance and transmittance of sample relative to the initial (blank) values or optical standards.	Monitoring transmittance of sample relative to the initial (blank) value.
Sample introduction	Manual sample introduction by a pushrod. Manual closing of the sample port.	Automatic sample introduction by a stepping motor. Automatic closure of the sample port.	Manual sample introduction by a long stem. Manual closing of the sample port.

Refining temperature in TOT/TOR analysis

J. C. Chow et al.

Title Page

Abstract | Introduction

Conclusions | References

Tables | Figures

|◄ | ►|

◄ | ►

Back | Close

Full Screen / Esc

Print Version

Interactive Discussion

EGU

Table 3. Summary of temperature calibration for five DRI Model 2001 thermal/optical carbon analyzers (CA #6–11).

Test Date	Tempilaq° G Temperature (°C)	121 ± 2	184 ± 2	253 ± 3	510 ± 6	704 ± 8	816 ± 9	• Slope(b)[d] • Intercept (a) • Number of Tests (n) • Correlation (r²)
11/2/04	DRI 2001 CA#6 $\overline{T}$ [a]	112	175	246	499	691	817	b = 0.995±0.004 a = 10.05±1.83 n = 24 (4x6)[e] r² = 0.996
	ΔT [b]	9 – 10	8 – 10	6 – 9	11 – 12	11 – 16	-4 – 1	
	$\overline{\Delta T} \pm \sigma_{\Delta T}$ [c]	9 ± 0.5	9 ± 1	7 ± 1	11 ± 1	13 ± 2	-1 ± 2	
2/11/04	DRI 2001 CA#7 $\overline{T}$ [a]	112	174	230	486	679	800	b = 1.012±0.005 a = 12.9±2.63 n = 24 (4x6)[e] r² = 0.999
	ΔT [b]	9 – 10	9 – 10	18 – 28	19 – 30	23 – 28	10 – 24	
	$\overline{\Delta T} \pm \sigma_{\Delta T}$ [c]	9 ± 1	10 ± 1	23 ± 4	24 ± 4	25 ± 2	16 ± 6	
21/4/04	DRI 2001 CA#9 $\overline{T}$ [a]	116	175	262	482	676	793	b = 1.040±0.009 a = -3.00±4.39 n = 18 (3x6)[e] r² = 0.998
	ΔT [b]	4 – 5	8 – 9	-10 – (-9)	26 – 29	26 – 29	22 – 24	
	$\overline{\Delta T} \pm \sigma_{\Delta T}$ [c]	5 ± 1	9 ± 1	9 ± 1	28 ± 2	28 ± 2	23 ± 1	
19/4/04	DRI 2001 CA#10 $\overline{T}$ [a]	113	174	239	495	678	794	b = 1.022±0.004 a = 6.55±2.15 n = 18 (3x6)[e] r² = 0.999
	ΔT [b]	7 – 9	8 – 14	13 – 16	12 – 19	17 – 34	17 – 25	
	$\overline{\Delta T} \pm \sigma_{\Delta T}$ [c]	8 ± 1	10 ± 3	14 ± 2	15 ± 4	26 ± 7	22 ± 4	
15/11/04	DRI 2001 CA#11 $\overline{T}$ [a]	116	179	246	490	683	807	b = 1.017±0.004 a = 4.28±1.95 n = 30 (5x6)[e] r² = 0.999
	ΔT [b]	4 – 5	5 – 6	6 – 7	18 – 21	20 – 24	9 – 10	
	$\overline{\Delta T} \pm \sigma_{\Delta T}$ [c]	5 ± 1	5 ± 1	7 ± 0.5	20 ± 1	21 ± 2	9 ± .05	

[a] $\overline{T}$ is the average measured temperature.

[b] ΔT is the difference between the rated Tempilaq° G (target) and thermocouple (measured) temperatures.

[c] $\overline{\Delta T} \pm \sigma_{\Delta T}$ indicates the average and standard deviation of ΔT

[d] Rated Tempilaq° G temperature (Y) versus thermocouple temperature (X).

[e] Number of replicates times the number of temperature plateaus.

Table 4. Summary of temperature calibration for five DRI/OGC thermal/optical carbon analyzers (CA #1–5).

Test Date	Tempilaq° G Indicator Temperature (°C)	121 ± 2	184 ± 2	253 ± 3	510 ± 6	704 ± 8	816 ± 9	• Slope (b)[d] • Intercept (a) • Number of Tests (n) • Correlation (r^2)
17/3/04	DRI/OGC CA#1 $\overline{T}$ [a]	84	147	209	469	637	N/A[c]	b = 1.028±0.028 a = 32.995±10.521 n = 10 (2×5)[e] r^2 = 0.994
	ΔT [b]	36 – 37	33 – 41	37 – 51	40 – 43	57 – 77	N/A	
18/3/04	DRI/OGC CA#2 $\overline{T}$ [a]	103	162	230	480	676	N/A	b = 1.017±0.005 a = 18.988±2.112 n = 10 (2×5)[e] r^2 = 0.999
	ΔT [b]	14 – 22	22 – 23	23 – 25	30 – 32	26 – 30	N/A	
22/3/04	DRI/OGC CA#3 $\overline{T}$ [a]	110	170	237	482	672	N/A	b = 1.037±0.009 a = 8.125±3.443 n = 10 (2×5)[e] r^2 = 0.999
	ΔT [b]	9 – 14	11 – 18	11 – 22	22 – 34	26 – 38	N/A	
23/3/04	DRI/OGC CA#4 $\overline{T}$ [a]	107	166	244	493	682	N/A	b = 1.012±0.007 a = 13.165±2.923 n = 10 (2×5)[e] r^2 = 0.999
	ΔT [b]	11 – 17	16 – 20	8 – 20	15 – 20	18 – 28	N/A	
24/3/04	DRI/OGC CA#5 $\overline{T}$ [a]	98	155	219	473	656	N/A	b = 1.036±0.010 a = 23.214±4.016 n = 10 (2×5)[e] r^2 = 0.999
	ΔT [b]	21 – 26	27 – 33	33 – 36	27 – 48	43 – 53	N/A	

[a] $\overline{T}$ is the average measured temperature.
[b] ΔT is the difference between the rated Tempilaq° G (target) and thermocouple (measured) temperatures.
[c] The DRI/OGC analyzer has a maximum temperature of 800°C.
[d] Rated Tempilaq° G temperature (Y) versus thermocouple temperature (X).
[e] Number of replicates times the number of temperature plateaus.

Refining temperature in TOT/TOR analysis

J. C. Chow et al.

EGU

Table 5. Summary of temperature calibration for the Sunset Laboratory Carbon Aerosol Analysis Laboratory Instrument.

Test Date	Tempilaq° G Temperature (°C)	121 ± 2	184 ± 2	253 ± 3	510 ± 6	649 ± 7	927 ± 9[f]	• Slope(b)[d] • Intercept (a) • Number of Tests (n) • Correlation (r²)
13/10/04	Sunset Inc. Instrument $\overline{T}$ [a]	95	152	253	519	619	912	b = 0.989±0.013 a = 20.32±6.72 n = 18 (3x6)[e] r² = 0.997
	ΔT[b]	24 – 29	32 – 33	-2 – 2	-11 – -7	29 – 30	12 – 17	
	$\overline{\Delta T} \pm \sigma_{\Delta T}$ [c]	26 ± 3	28 ± 1	0 ± 2	-9 ± 2	30 ± 3	15 ± 3	

[a] $\overline{T}$ is the average measured temperature.

[b] ΔT is the difference between the rated Tempilaq° G (target) and thermocouple (measured) temperatures.

[c] $\overline{\Delta T} \pm \sigma_{\Delta T}$ indicates the average and standard deviation of ΔT

[d] Rated Tempilaq° G temperature (Y) versus thermocouple temperature (X).

[e] Number of replicates times the number of temperature plateaus.

[f] The 927 °C standard was used in place of the 816 °C standard to better represent the larger temperature range spanned by the HKUST-3 temperature protocol.
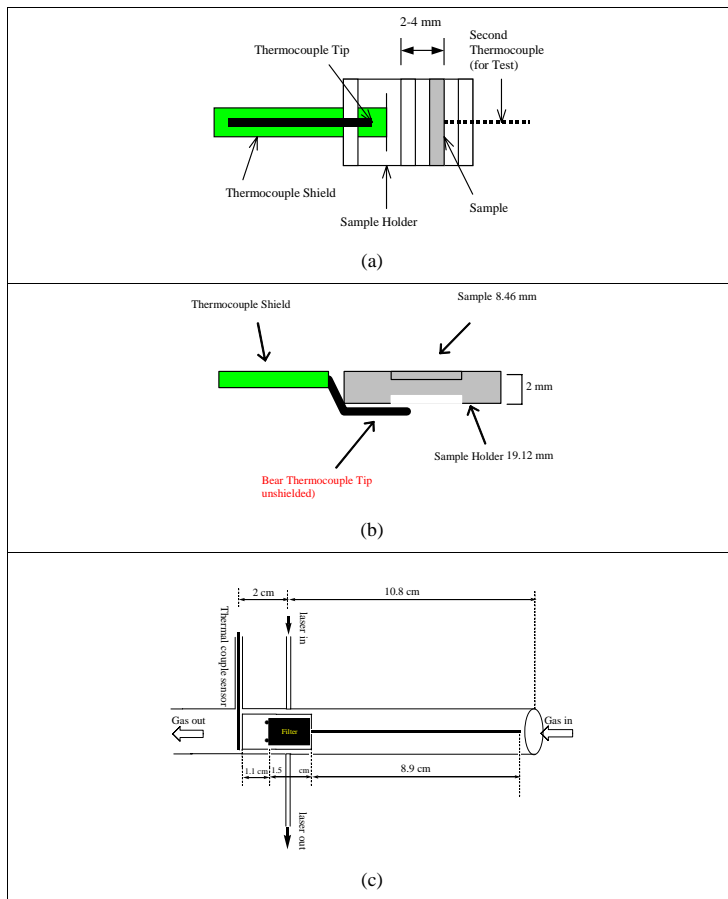
Fig. 1. Schematic diagram of sample holder design for the: **(a)** Desert Research Institute/Oregon Graduate Center (DRI/OGC) carbon analyzer, **(b)** DRI Model 2001 thermal/optical carbon analyzer; and **(c)** Sunset Laboratory Carbon Aerosol Analysis Laboratory Instrument.
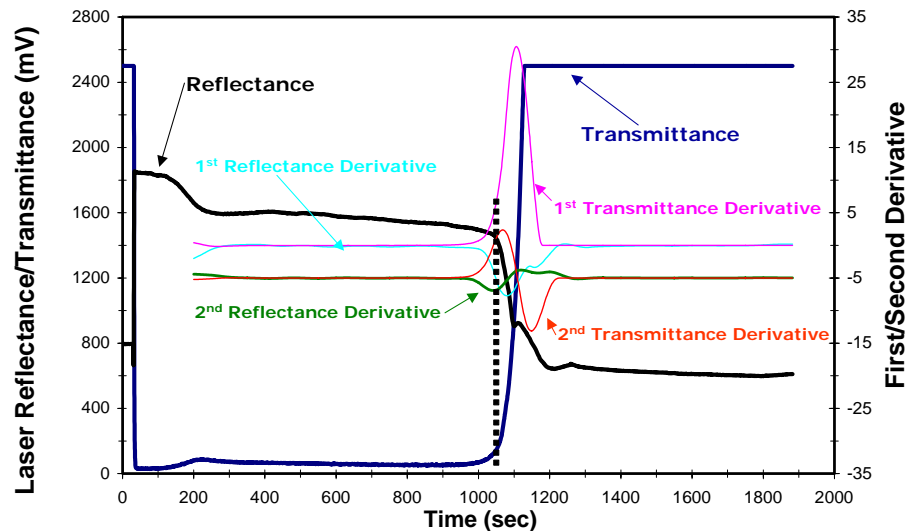
EGU
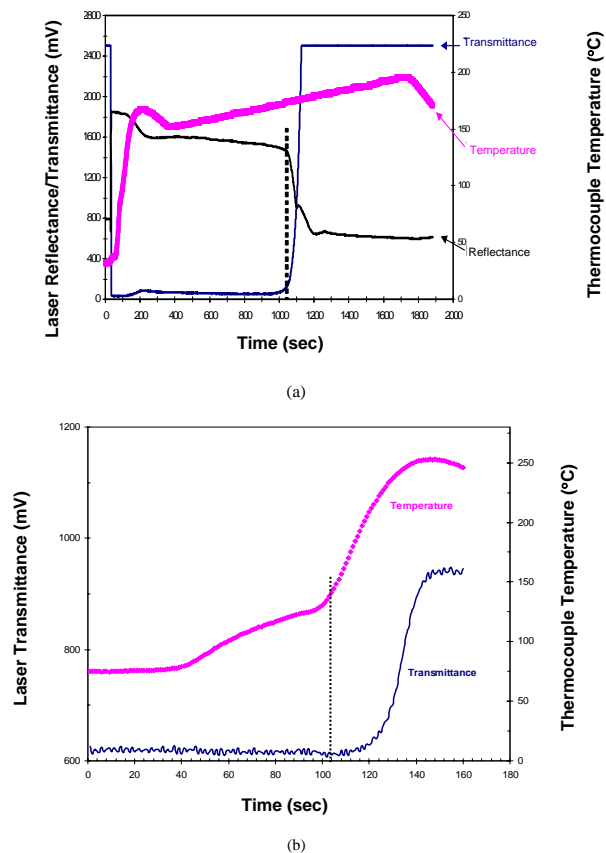
Fig. 2. Temperature ramping with a Tempilaq° G temperature indicator rated at 184°C for the: **(a)** DRI Model 2001; and **(b)** Sunset Laboratory carbon analyzers. Also shown are reflectance and transmittance of the temperature indicator (if available). The vertical dashed line indicates the achievement of the rated temperature.

EGU

(Tempilaq's melting point 184 ± 2 °C)

Fig. 3. Reflectance and transmittance measurements and their first and second derivatives over time with a Tempilaq° G temperature indicator rated at 184°C (Fig. 2). The vertical dashed line indicates the achievement of the rated target temperature.
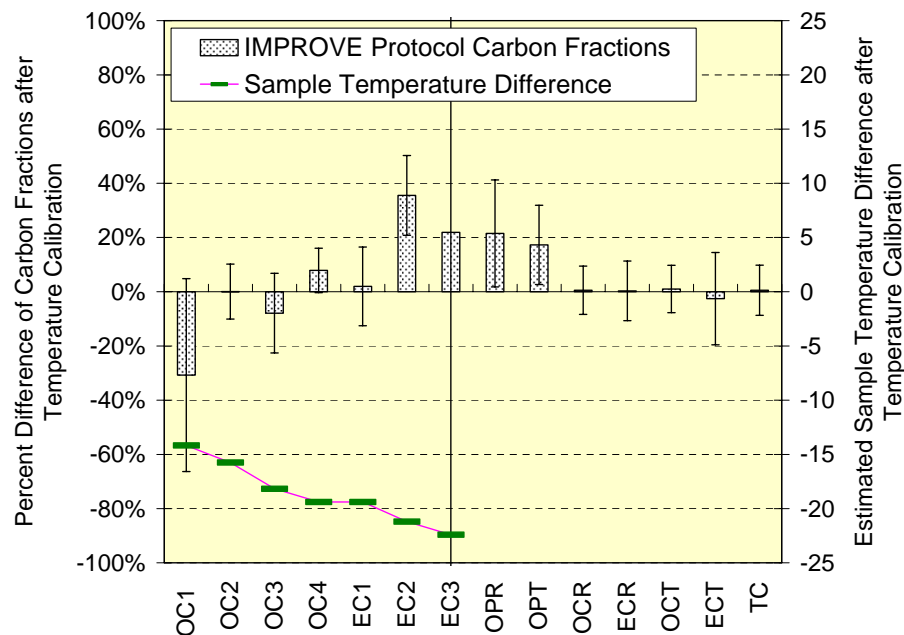
EGU
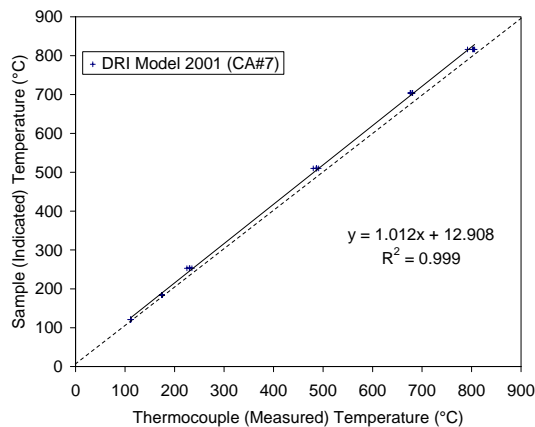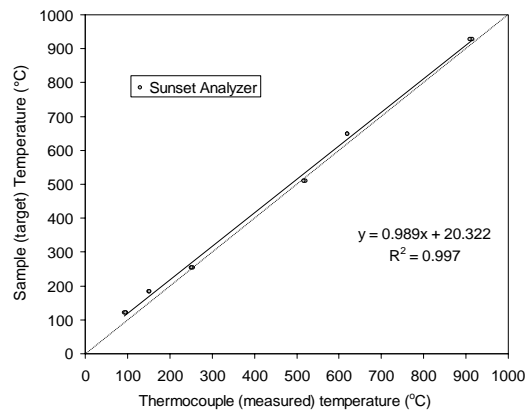
Fig. 4. Linear regression of sample (target) temperature against thermocouple (measured) temperature for the: **(a)** DRI Model 2001 (CA #7); and **(b)** Sunset Laboratory carbon analyzers.

Fig. 5. Changes in carbon fractions after adjustment for temperature calibration (Fig. 4) with DRI Model 2001 thermal/optical carbon analyzer (CA#7). Statistics are based on average and standard deviation of analysis results of five ambient samples from the Fresno Supersite (TC: 3.5–15 μg m^{-3}). Sample (target) temperature is lowered by 14 to 22°C after the calibration. Carbon fractions are defined in Table 1.

EGU